J|A|C|S
JOURNAL OF THE AMERICAN CHEMICAL SOCIETY
Article
pubs.acs.org/JACS

Unexpected Consequences of Block Polydispersity on the Self-Assembly of ABA Triblock Copolymers

Joan M. Widin, Adam K. Schmitt, Andrew L. Schmitt, Kyuhyun Im, and Mahesh K. Mahanthappa*

Department of Chemistry, University of Wisconsin—Madison, 1101 University Avenue, Madison, Wisconsin 53706, United States

Supporting Information

ABSTRACT: Controlled/"living" polymerizations and tandem polymerization methodologies offer enticing opportunities to enchain a wide variety of monomers into new, functional block copolymer materials with unusual physical properties. However, the use of these synthetic methods often introduces nontrivial molecular weight polydispersities, a type of chain length heterogeneity, into one or more of the copolymer blocks. While the self-assembly behavior of monodisperse AB diblock and ABA triblock copolymers is both experimentally and theoretically well understood, the effects of broadening the copolymer molecular weight distribution on block copolymer phase behavior are less well-explored. We report the melt-phase self-assembly behavior of SBS triblock copolymers (S = poly(styrene) and B = poly(1,4-butadiene)) comprised of a broad polydispersity B block (M_w/M_n = 1.73−2.00) flanked by relatively narrow dispersity S blocks (M_w/M_n = 1.09−1.36), in order to identify the effects of chain length heterogeneity on block copolymer self-assembly. Based on synchrotron small-angle X-ray scattering and transmission electron microscopy analyses of seventeen SBS triblock copolymers with poly(1,4-butadiene) volume fractions $0.27 \leq f_B \leq 0.82$, we demonstrate that polydisperse SBS triblock copolymers self-assemble into periodic structures with unexpectedly enhanced stabilities that greatly exceed those of equivalent monodisperse copolymers. The unprecedented stabilities of these polydisperse microphase separated melts are discussed in the context of a complete morphology diagram for this system, which demonstrates that narrow dispersity copolymers are not required for periodic nanoscale assembly.

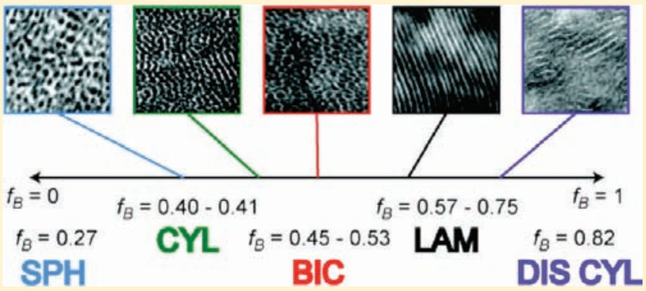

■ INTRODUCTION

Self-assembly at length scales ranging from that of molecules to colloids to macroscopic objects furnishes access to a variety of functional and technologically useful materials.[1] Control over the morphologies and stabilities of these self-assembled structures may be achieved by chemically tailoring the size, shape, and interactions of their constituents, in order to tune the bulk materials properties. Well-known examples of such systems include quantum dot superlattices with unique electronic and optical properties,[2−4] mesoscale self-assembly of macroscopic objects,[5,6] soft colloidal self-assembly,[7,8] and bulk and thin-film block copolymer self-assembly.[9−12] By virtue of the apparent similarities between thermodynamic self-assembly and small-molecule crystallization processes, uniformity in the size and shape of the self-assembling objects is commonly considered a prerequisite for formation of structurally periodic ensembles; irregularly shaped objects of variable sizes do not generally pack into well-ordered structures.[1] Only a few studies of molecular self-assembly have questioned the validity and stringency of the assumption that low degrees of heterogeneity are necessary for periodic structure formation.[13−16]

Block copolymers, molecules derived from covalently bonding two or more chemically incompatible homopolymer segments, comprise a prototypical set of useful, commodity materials whose special properties crucially depend upon their self-assembly at the nanoscale.[9,11] The melt-phase self-assembly of AB diblock and ABA triblock copolymers into periodically ordered nanoscale structures reflects a delicate balance between the enthalpy of interaction between dissimilar monomer segments and the configurational entropy loss due to chain stretching that minimizes unfavorable monomer contacts. The theoretical phase behavior of perfectly monodisperse AB diblock copolymers is parametrized by the volume fraction of the A block $f_A = 1 - f_B$ and the product $\chi_{AB}N$, where χ_{AB} quantifies the enthalpy associated with unfavorable A−B monomer contacts (which depends inversely on temperature T), and N is the total degree of polymerization of the copolymer.[17] Leibler[18] calculated the expected microphase separation behavior of perfectly monodisperse AB diblock copolymers as a function of these order parameters and predicted the compositions at which lamellar, cylindrical, and spherical morphologies are stable (Scheme 1). An important result of this theory is the prediction of a critical $\chi_{AB}N$ above which AB diblock copolymers microphase separate. This critical value specifies the composition-dependent order-to-disorder transition temperature (T_{ODT}), at which the self-assembled

Received: November 10, 2011
Published: January 17, 2012

Scheme 1. Equilibrium Morphologies Adopted by ABA Triblock Copolymers

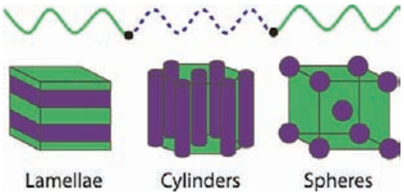

structure "melts" into an unstructured fluid. For AB diblock copolymers, microphase separated structures are observed only when $\chi_{\mathrm{AB}}N \geq 10.495$.[18] Experiments employing block copolymers with relatively low dispersities ($M_w/M_n \leq 1.1$) largely agree with these morphological and thermodynamic predictions, although more sophisticated theories[19−21] have been developed to account for newer observations.[22−25] Mayes and Olvera de la Cruz have extended Leibler's mean-field theory to show that melt microphase separation in ABA triblock copolymers requires $\chi_{\mathrm{AB}}N \geq 17.9$.[26,27]

Advances in tandem and controlled polymerizations have enabled access to a plethora of new block copolymers with variable molecular weights, molecular weight distributions, and compositions.[28−32] These new synthetic methods enable the enchainment of functional monomers that endow the resulting copolymers with unusual thermal, optical, electronic, and permselective properties. However, use of these polymerization techniques to produce block copolymers often comes at the expense of introducing significant molecular weight polydispersity into one or more of the copolymer blocks.[33−39] Therefore, the development of new materials derived from these advanced polymerization methods motivates fundamental studies of the effects of block polydispersity on the nanoscale self-assembly behavior of these designer soft materials.

Several groups have recently investigated the role of continuous block polydispersity on the microphase separation behavior of AB, BAB, and ABC block copolymers.[13−16,40−47] In poly(styrene-*block*-acrylic acid) diblock copolymers derived from reversible-addition fragmentation chain transfer (RAFT) polymerizations, Bendejacq et al. found that polydispersity in both blocks still allows the formation of classical spheres, cylinders, and lamellar morphologies.[13] For AB diblock copolymers comprised of a narrow dispersity A block ($M_w/M_n \leq 1.05$) and a variable dispersity B block (M_w/M_n = 1.18−2.00), Lynd and Hillmyer observed shifts in the composition-dependent microphase windows consistent with increased interfacial curvature toward the polydisperse segment. They also observed microdomain dilation with increasing polydispersities.[15] Furthermore, they reported a polymer composition-dependent (de)stabilization of polydisperse microphase separated melts as compared to their narrow dispersity analogs.[48] A report by Ruzette et al. on the microphase separation behavior of acrylic BAB triblocks comprised of polydisperse B blocks flanking relatively narrow dispersity A blocks coheres with the aforementioned studies.[14] Recent studies by Register and co-workers of polyolefin AB diblock copolymers derived from "chain shuttling" coordination−insertion polymerization, in which *both* segments are polydisperse, have demonstrated large increases in the characteristic supramolecular domain spacings as well as increased values of T_{ODT}.[46] However, all of these studies concern the self-assembly behavior of polydisperse block copolymers in which a polydisperse segment is tethered to a block junction at only one end, leaving the other end free (Figure 1a,b).

Constraining the polydisperse B segment in the middle of an ABA copolymer chain, such that its ends are pinned at two block junctions (Figure 1c), may be expected to alter its microphase separation behavior as compared to the aforementioned BAB triblocks with polydisperse end blocks (Figure 1b). However, the physical consequences of incorporating a polydisperse B block in the center of an ABA triblock copolymer are poorly understood, in spite of established synthetic routes to such polymers.[33,35,36,39,49] Since conventional wisdom suggests that narrow dispersity is a requirement for supramolecular self-assembly,[41] these copolymers have remained largely unstudied and underutilized.[35,36,50] This preconceived notion concerning polydisperse block copolymer self-assembly has led synthetic polymer chemists to spurn polymer syntheses that yield unimodal multiblock copolymers with broader polydispersities ($M_w/M_n \geq 1.3$).

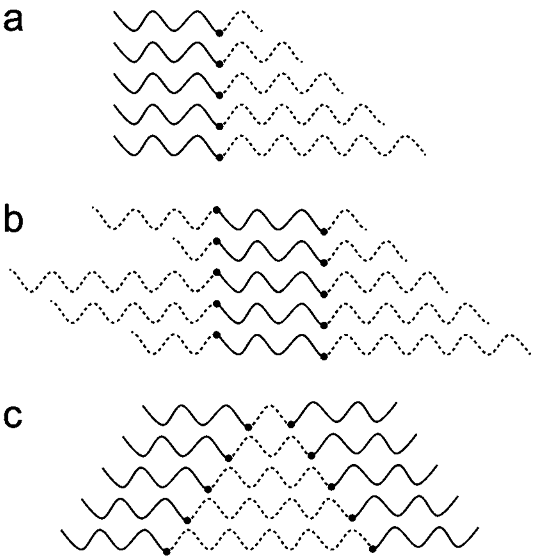

Figure 1. (a) AB diblocks and (b) BAB triblocks with polydisperse B blocks at the chain ends self-assemble differently from (c) ABA triblocks, in which the polydisperse segment is constrained at two block junctions.

In order to explore the effects of polydisperse block connectivity on copolymer self-assembly, we have used an optimized combination of ring-opening metathesis polymerization with chain transfer (ROMP-CT) and atom transfer radical polymerization (ATRP)[50] to synthesize a series of model poly(styrene-*block*-1,4-butadiene-*block*-styrene) (SBS) triblock copolymers having polydisperse center B blocks (M_w/M_n = 1.73−2.00) and narrow dispersity outer S blocks (M_w/M_n = 1.09−1.36). Near symmetric compositions ($f_B \sim 0.50$), we previously reported that these polydisperse block copolymers microphase separate into a thermally stable, disordered bicontinuous morphology that persists at very low molecular weights and segregation strengths ($\chi_{\mathrm{AB}}N < 6.5$); whereas, analogous narrow dispersity materials are disordered fluids.[50] Building upon this initial observation, we report the morphology diagram for these polydisperse SBS triblock copolymers with $0.27 \leq f_B \leq 0.82$. We specifically show that B segment polydispersity causes dramatic shifts in the composition-dependent morphology windows of SBS triblock copolymers, while enabling their self-assembly into unexpectedly stable periodic structures as compared to their monodisperse analogs. These results highlight the unusual consequences of block polydispersity and chain connectivity on SBS triblock copolymer self-assembly.

■ RESULTS AND DISCUSSION

Synthesis and Molecular Characterization. Poly(styrene-*block*-1,4-butadiene-*block*-styrene) (SBS) triblock copolymers were synthesized using our previously reported procedure shown in Scheme 2.[50] Chain transfer ring-opening metathesis polymerization (ROMP-CT)[52] of purified 1,5-cyclooctadiene (1,5-COD)[53] in the presence of *trans*-1,4-dibromo-2-butene catalyzed by Grubbs' second generation metathesis catalyst (IMes)RuCl$_2$(CHPh)(PCy$_3$) in toluene at 22 °C yielded a series of telechelic α,ω-dibromo-poly(1,4-butadiene) (B) homopolymers with $M_{n,B}$ = 6.1−20.2 kg/mol and polydispersity indices M_w/M_n = 1.73−2.00. The close agreement between $M_{n,B}$ determined by size-exclusion chromatography (SEC) and ^{1}H NMR polymer end group analyses indicates a high degree of allylic bromide chain end functionality ($F_n \approx 2.0$) per our previous report. α,ω-dibromo-poly(1,4-butadiene) telechelics served as macroinitiators for the copper(I)-catalyzed atom-transfer radical polymerization (ATRP) of styrene at 110 °C to yield polydisperse yet unimodal SBS triblock copolymers with M_w/M_n = 1.42−1.86 (see Supporting Information for details).[50] Cross-metathesis degradation of SBS triblock copolymers using 1-hexene[49] enabled the isolation and direct characterization of the S homopolymer end blocks, thus allowing the complete characterization of the molecular weight distributions of each block in these copolymers. The S blocks exhibit narrow polydispersities M_w/M_n = 1.09−1.36 according to SEC analyses. Figure 2 shows an overlay of SEC traces associated with SBS-12.3-53, including the B telechelic, the SBS triblock, and the S end blocks isolated from cross-metathesis degradation. The thermal stabilities of these polymers were dramatically enhanced by removal of ATRP catalyst residues by elution of polymer/THF solutions through basic alumina and by the addition of the antioxidant Irganox 1076 (≤1 wt %). The complete molecular characteristics of the seventeen triblocks examined in this study with 0.27 ≤ f_B ≤ 0.82 are given in Table 1. Samples are identified as SBS-X-Y, where X is the total M_n (kg/mol) and Y is the poly(1,4-butadiene) volume percentage (f_B) calculated from quantitative ^{1}H NMR and the respective homopolymer melt densities at 140 °C.[51]

Scheme 2. Tandem ROMP-ATRP Synthesis of Polydisperse, Unimodal SBS Triblock Copolymers

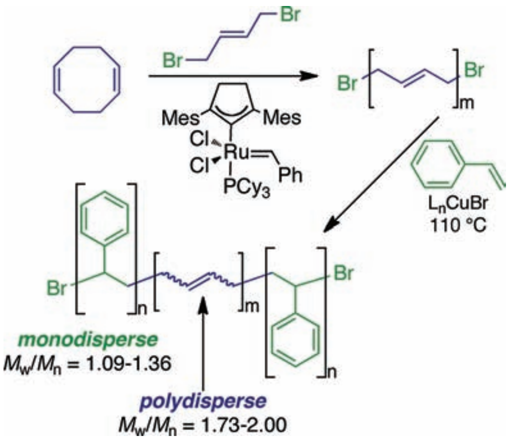

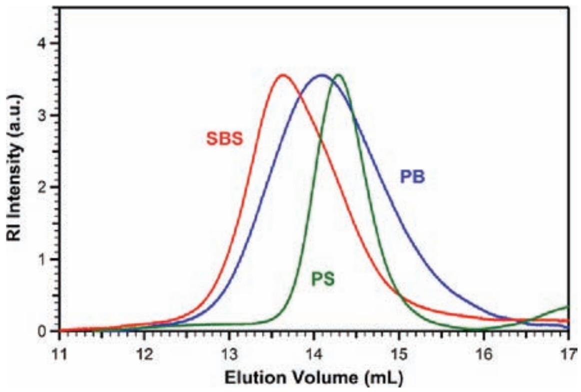

Figure 2. Sample SEC traces for SBS-12.3-53 showing the polydisperse telechelic α,ω-poly(1,4-butadiene) (blue), polydisperse SBS triblock copolymer (red), and the S end block isolated from cross-metathesis degradation of the SBS triblock copolymer (green).

The Lamellar Window: 0.57 ≤ f_B ≤ 0.75. SBS triblock copolymers with 0.57 ≤ f_B ≤ 0.75 and a polydisperse center B block adopt a lamellar morphology (Table 2 and Figure 3). Between T = 22−160 °C, SBS samples with compositions near the center of this phase window exhibit small-angle X-ray scattering (SAXS) maxima at q^*, $2q^*$, and $3q^*$ that correspond to the (100), (200), and (300) Bragg reflections of a lamellar phase. The Bragg reflections of SBS-19.2-61 disappear above 160 °C, as the supramolecular layered structure melts into an isotropic liquid. SBS-19.2-61 thus exhibits an accessible T_{ODT} = 160 °C, above which only a single, correlation-hole SAXS peak characteristic of a disordered block copolymer melt is observed.[54] SBS-29.1-65 also exhibits T_{ODT} = 150−170 °C with a broader transition to the disordered state, evidenced by the appearance of a single correlation-hole SAXS peak (see Supporting Information Figure S1). All other samples in this composition window remain microphase separated up to 220 °C (above which polymer decomposition occurs). Near the edges of the lamellar phase window, SAXS patterns for SBS-30.2-57 and SBS-27.0-75 show only two broad reflections at q^* and $2q^*$ with no evidence for higher order scattering maxima. This scattering signature is indicative of both reduced translational order and larger deviations in the lamellar periods of these morphologies.[55]

TEM analyses corroborate the lamellar morphology assignments for these samples derived from SAXS (insets in Figure 3). TEM samples were cryo-microtomed at −150 °C and the poly(1,4,-butadiene) domains were selectively stained at 22 °C with OsO$_4$ vapor for enhanced imaging contrast. Real-space images of SBS-29.1-65 and SBS-29.2-72 confirm that these samples exhibit long-range lamellar order with subtle variations in the domain spacing, in accordance with the observed extinction of the higher order SAXS peaks. We ascribe these slight variations in the lamellar period to the broad polydispersity of the center B block. SBS-27.0-75 exhibits wider variations in the lamellar thickness as surmised by SAXS, suggesting the onset of debinding of these lamellae due to the presence of a larger polydisperse B block. At the opposite end of this composition range, images of SBS-30.2-57 show the formation of defective lamellae with reduced translational order that we attribute to the proximity of this sample to a phase

Table 1. Molecular Characteristics of SBS Triblock Copolymers

	SBS Triblock					B Block		S Block	
	$M_{n,\text{total}}$ (kg/mol)[e]	PDI[b]	w_B	f_B[c]	N[d]	$M_{n,\text{SEC}}$ (kg/mol)[a]	PDI[a]	$M_{n,\text{ NMR}}$ (kg/mol)[e]	PDI[b]
				Polydisperse					
SBS-28.6-27	28.6	1.42	0.24	0.27	433	6.8	1.91	10.9	1.30
SBS-33.8-40	33.8	1.50	0.32	0.40	553	11.0	1.98	11.4	1.11
SBS-35.8-41	35.8	1.50	0.37	0.41	551	13.2	1.73	11.3	1.36
SBS-36.8-45	36.8	1.60	0.41	0.45	571	15.0	2.00	10.9	1.16
SBS-36.1-48	36.1	1.40	0.44	0.48	564	16.0	1.90	10.1	*n.d.*[f]
SBS-35.5-49	35.5	1.57	0.45	0.49	555	16.0	1.90	9.8	1.20
SBS-32.9-51	32.9	1.63	0.46	0.51	517	15.3	1.79	8.8	*n.d.*[f]
SBS-12.3-53	12.3	1.60	0.49	0.53	194	6.1	1.90	3.2	1.09
SBS-30.2-57	30.2	1.66	0.53	0.57	478	16.0	1.90	7.1	1.25
SBS-35.6-59	35.6	1.64	0.55	0.59	566	19.6	1.93	8.0	1.23
SBS-19.2-61	19.2	1.75	0.57	0.61	305	11.0	1.98	4.1	*n.d.*[f]
SBS-29.1-65	29.1	1.75	0.61	0.65	467	17.7	1.99	5.7	1.11
SBS-29.2-72	29.2	1.80	0.69	0.72	475	20.2	1.88	4.5	1.34
SBS-27.0-75	27.0	1.82	0.72	0.75	442	19.6	1.93	3.7	1.20
SBS-18.4-77	18.4	1.83	0.74	0.77	302	13.6	1.94	2.4	1.14
SBS-25.4-82	25.4	1.86	0.79	0.82	419	20.2	1.88	2.6	1.25
SBS-22.7-83	22.7	1.85	0.81	0.83	376	18.3	1.81	2.2	*n.d.*[f]
				Monodisperse					
mSBS-30.6-52	36.1	1.05	0.48	0.52	481	14.6	*n.d.*[f]	8.0	1.09
mSBS-32.1-68	32.1	1.06	0.65	0.68	503	20.2	*n.d.*[f]	5.5	1.12

[a] PDI = M_w/M_n; determined by size exclusion chromatography (SEC) in THF at 40 °C using a Mark−Houwink corrected polystyrene calibration for poly(1,4-butadiene). [b] Determined by size exclusion chromatography (SEC) in THF at 40 °C using polystyrene calibration. [c] Volume fraction of poly(1,4-butadiene) calculated using the homopolymer melt densities at 140 °C.[51] [d] Calculated using a 118 Å^3 monomer reference volume. [e] Calculated from quantitative ^{1}H NMR spectra of the copolymers using the $M_{n,B}$. [f] not determined.

Table 2. Morphological Characteristics of SBS Triblock Copolymers

Sample	N	Phase[a]	d (nm)[b]
SBS-28.6-27	433	SPH	*n.d.*[c]
SBS-33.8-40	553	HEX	28.9
SBS-35.8-41	551	HEX	35.4
SBS-36.8-45	571	BIC	30.6[d]
SBS-36.1-48	564	BIC	39.8[d]
SBS-35.5-49	555	BIC	39.8[d]
SBS-32.9-51	517	BIC	39.5[d]
SBS-12.3-53	194	BIC	39.3[d]
SBS-30.2-57	478	LAM	37.4[d]
SBS-35.6-59	566	LAM	60.4
SBS-19.2-61	305	LAM	28.8
SBS-29.1-65	467	LAM	35.9
SBS-29.2-72	475	LAM	43.4
SBS-27.0-75	442	LAM	60.4
SBS-18.4-77	302	DIS	*n.d.*[c]
SBS-25.4-82	419	DIS CYL	35.5[e]
SBS-22.7-83	376	DIS	*n.d.*[c]
Monodisperse			
mSBS-30.6-52	481	LAM	18.7
mSBS-32.1-68	503	HEX	19.7

[a] Determined by either SAXS, TEM, or a combination of these methods. [b] Principal domain spacing calculated as $d = 2\pi/q^*$, where the magnitude of the principal scattering wavevector q^* is determined from SAXS at 140 °C. [c] not determined. [d] Calculated from SAXS at 150 °C. [e] Calculated from SAXS at 90 °C.

boundary. This observation is reinforced by the appearance of a broad shoulder in the SAXS pattern situated between the q^* and $2q^*$ scattering peaks.

The above data taken together imply that B block polydispersity dramatically shifts the position of the lamellar composition window for ABA triblock copolymers. Monodisperse ABA triblocks typically exhibit a cylindrical morphology between f_B = 0.65−0.80, in which hexagonally ordered A-rich cylinders are embedded in a B-rich matrix phase, while lamellae are typically observed in the range f_B = 0.35−0.65.[26,56] The above data show that lamellae are formed by polydisperse SBS copolymers only when $0.57 \leq f_B \leq 0.75$. This result is consistent with recent observations by Schmitt and Mahanthappa indicating that midblock polydispersity shifts the lamellar phase window in related poly(ethylene oxide-*block*-1,4-butadiene-*block*-ethylene oxide) triblock copolymers to higher f_B.[39] Since lamellar phases form when the volumes occupied by the two constituent homopolymers are nearly equal, the last statement implies that the polydisperse B block fills a smaller volume than expected based on $M_{n,B}$. Thus, we conclude that the interfaces of the microphase separated morphology curve toward the polydisperse segment in a manner consistent with prior results for AB and BAB copolymers containing polydisperse B segments.[14,15] However, we ascribe the much larger lamellar phase window shift for our SBS triblocks to the chain architecture, wherein the polydisperse B segment is constrained at both ends as an interior segment in the copolymer chain.

The characteristic domain spacings of polydisperse SBS triblocks are also substantially greater than those of monodisperse materials of comparable total molecular weights (Table 1). For example, the cylindrical morphology adopted by monodisperse and compositionally similar mSBS-32.1-68 has a characteristic domain spacing $d \sim 20$ nm (Table 2), which is significantly smaller than d = 36−43 nm observed for the lamellae-forming polydisperse SBS-29.1-65 and SBS-29.2-72.

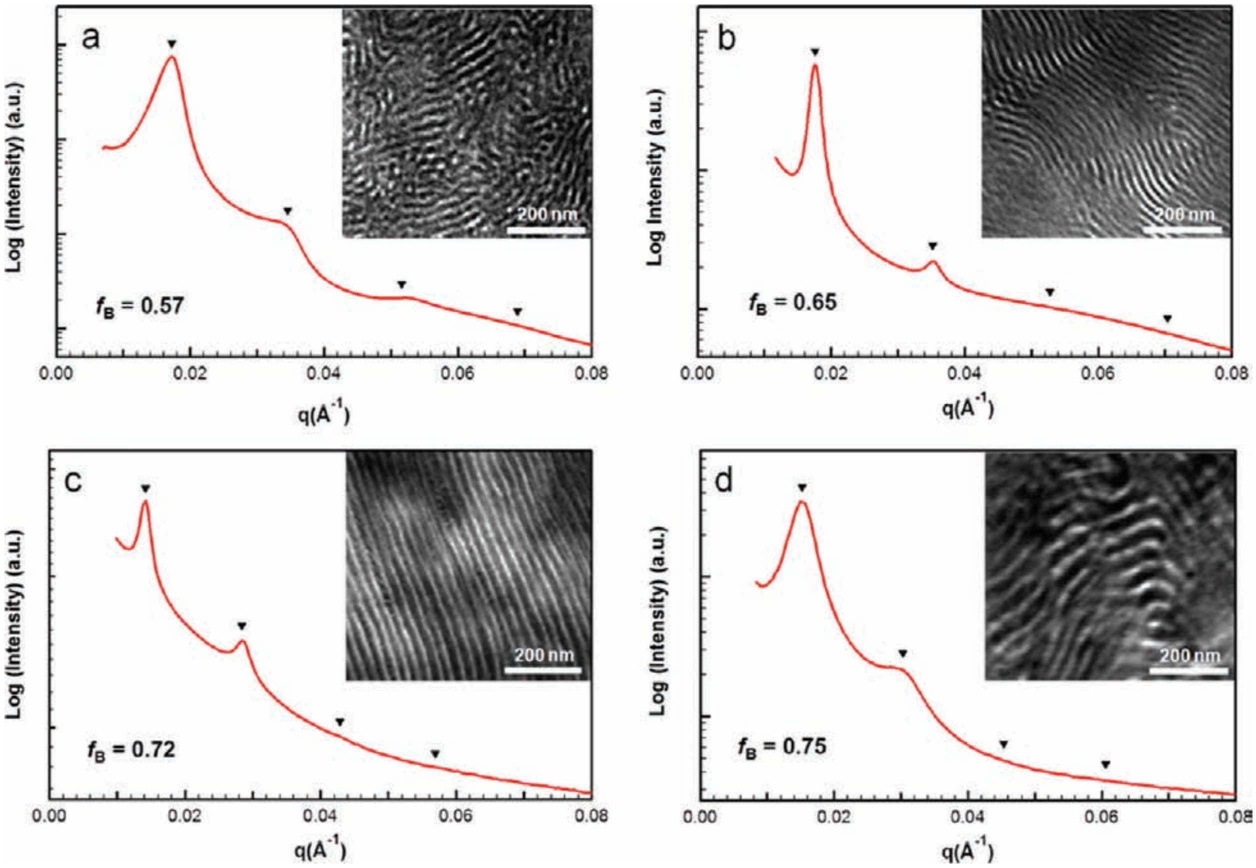

Figure 3. Azimuthally integrated synchrotron SAXS patterns for (a) SBS-30.2-57 at 120 °C, (b) SBS-29.1-65 at 110 °C, (c) SBS-29.2-72 at 150 °C, and (d) SBS-27.0-75 at 120 °C, with markers indicating the expected peak positions for a lamellar morphology based on the position of the primary scattering wavevector (q^*). Insets show representative TEM micrographs for each sample annealed at 130 °C for 24 h, which were stained with OsO_4 so that the poly(1,4-butadiene) domains appear dark.

Monodisperse mSBS-30.6-52 exhibits a lamellar morphology with d = 18.7 nm at $M_{n,total}$ = 36.1 kg/mol, which is also much smaller than that observed for any of the polydisperse lamellar SBS samples (SBS-30.2-57 to SBS-27.0-75). Domain dilation by virtue of segmental polydispersity in block copolymers has been previously attributed to the combination of chain length polydispersity and composition polydispersity in samples exhibiting continuous molecular weight distributions (Figure 1).[14,39,46,57] We return to the detailed origins of this phenomenon below, after describing the complete morphological behavior of these polydisperse SBS materials.

The remarkable thermal stabilities of the *polydisperse* SBS lamellar phases, evidenced by $T_{ODT} \geq 220$ °C for many samples, imply that the minimum segregation strength for microphase separation is $\chi_{SB}N \geq 9.5$ (*vide infra*). Mean-field theory calculations by Mayes and Olvera de la Cruz,[27] and experiments by Ryan and co-workers[56] indicate that microphase separation in *monodisperse* ABA triblock copolymers requires a critical segregation strength $\chi N \geq 17.9$. Therefore, we conclude that B segment polydispersity in ABA triblock copolymers lowers the critical χN for microphase separation, implying microphase-separated melt stabilization. While Lynd and Hillmyer did observe modest stabilization of their microphase separated morphologies upon increasing the polydispersity of one homopolymer segment in AB diblock copolymers,[48] substantially greater thermodynamic stabilization is observed here for SBS triblocks with a polydisperse interior block.

Disordered Bicontinuous Phase: $0.45 \leq f_B \leq 0.53$. We previously reported a series of five SBS triblock copolymers with polydisperse center blocks ($M_{n,total}$ = 12.3−30.6 kg/mol) and nearly symmetric volume fractions ($f_B \approx 0.50$), which exhibit an unusually stable disordered bicontinuous morphology with T_{ODT}'s well above the polymer decomposition temperature (~220 °C).[50] We showed that this microphase separated morphology exhibits a distinct SAXS signature that does not match any known, well-ordered morphology. The observed principal domain spacings (d) for these samples depend only weakly on $M_{n,total}$ ($d \sim N^0$), in contrast to monodisperse microphase separated block copolymers for which $d \sim N^{2/3}$ at high segregation strengths. In our previous paper, we speculated that the observed invariance of d on $M_{n,total}$ stems from the fact that only the longest chains in these broad dispersity samples dictate the characteristic microdomain spacing.[50] While the exact origins of this effect are somewhat obscure, recent reports on olefin block copolymers from "chain-shuttling" polymerization catalysis[58] have also noted a similarly weak dependence of d on $M_{n,total}$.[43,46] Melt rheological analyses of these SBS copolymers established that their microphase separated structures bear similarities to bicontinuous microemulsions[59,60] and other known bicontinuous morphologies,[34] which can be stabilized by macromolecular polydispersity.[61]

Thorough morphological studies of SBS-12.3-53 and SBS-36.8-45 establish that the composition window for the disordered bicontinuous morphology spans the range f_B = 0.45−0.53. Synchrotron SAXS analyses indicate a low-level of nanoscale order in these polymer melts, inferred by the absence of higher order SAXS peaks and their large full-widths at half-maximum (Figure 4). Attempts to solvent cast these samples from a good solvent (e.g., toluene or tetrahydrofuran), to anneal them at high temperatures for extended periods, or to shear orient these polymer melts in a parallel-plate rheometer failed to induce better long-range order in these samples. TEM images reveal similar web-like features characteristic of a disordered bicontinuous morphology consisting of interpenetrating S and B domains (Figure 4 insets). These images also illustrate a pronounced tendency for the microphase-separated interfaces to curve toward the polydisperse polybutadiene domains.

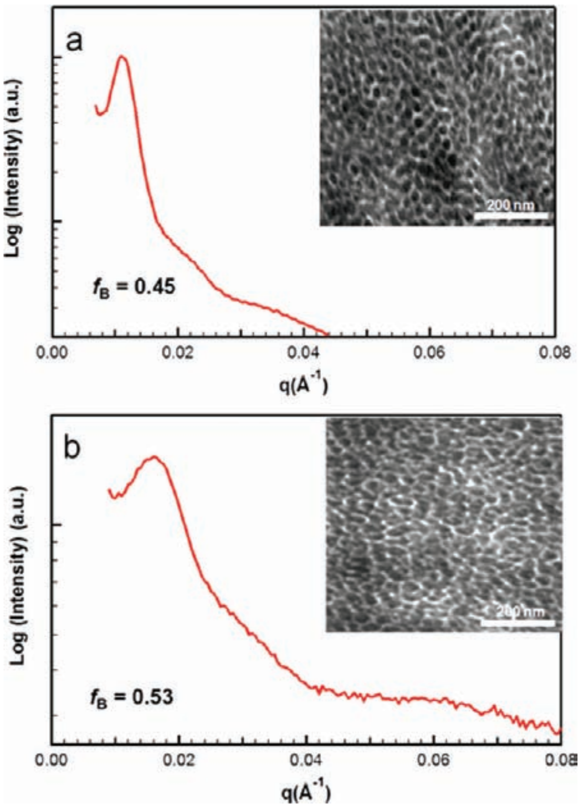

Figure 4. Azimuthally integrated (a) synchrotron SAXS pattern for SBS-36.8-45 at 170 °C, and (b) lab source SAXS pattern for SBS-12.3-53 at 150 °C, along with insets showing TEM images of the disordered bicontinuous morphology adopted by both samples.

Ordered samples with f_B = 0.27–0.41. SBS triblock copolymers with $f_B \sim 0.40$ and $\chi_{SB}N = 15.5$ adopt cylindrical morphologies, in which cylinders of the polydisperse B segment are ordered on a two-dimensional hexagonal lattice within a narrow dispersity polystyrene matrix. A sample SAXS pattern for SBS-33.8-40 at 180 °C shows three peaks at q^*, $\sqrt{3}q^*$, and $2q^*$ characteristic of a cylindrical morphology with a very low degree of long-range translational order (Figure 5a); TEM images of this sample also show local hexagonal order (inset Figure 5a). In spite of the slightly broader S block polydispersity (M_w/M_n = 1.36) associated with SBS-35.8-41, this sample exhibits Bragg reflections by SAXS located at q^*, $\sqrt{3}q^*$, $2q^*$, and a much weaker peak at $\sqrt{7}q^*$ also consistent with a cylindrical morphology (Figure 5b). TEM images support this morphological assignment, although the semicrystalline nature of the B block disrupts the morphology to some extent. The morphologies adopted by these samples are reminiscent of those recently reported by Wagner et al. for polydisperse polycarbonate-based block copolymers derived from segment-interchange olefin metathesis polymerizations.[62]

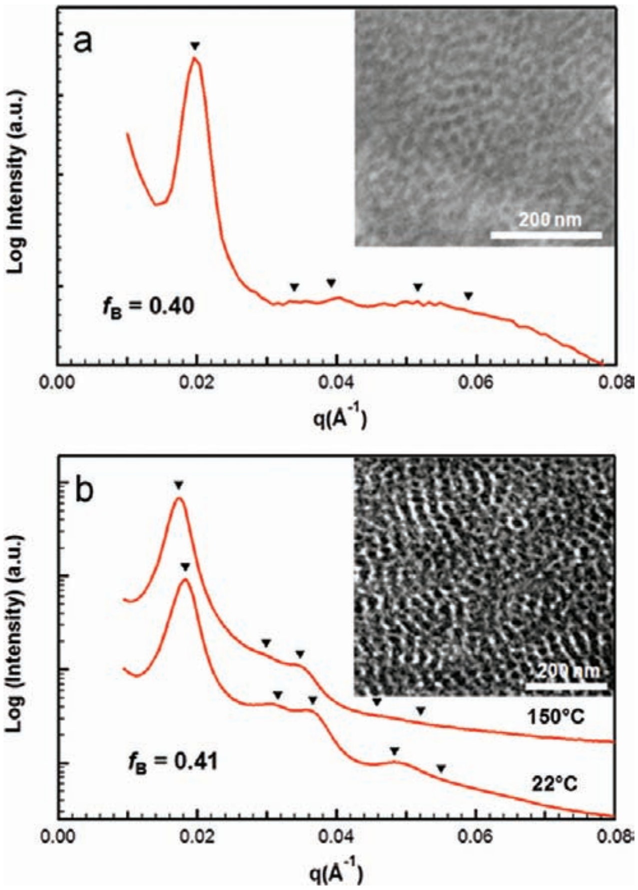

Figure 5. (a) Azimuthally integrated synchrotron SAXS pattern for SBS-33.8-40 at 180 °C with markers indicating the calculated peak positions for a hexagonally packed cylinders morphology, and an inset showing a TEM micrograph of the sample. (b) Azimuthally integrated synchrotron SAXS patterns for SBS-35.8-41 at 22 °C (bottom) and 150 °C (top) that was sheared in a parallel-plate rheometer at 160 °C, which exhibit peaks consistent with a hexagonally packed cylinders morphology, along with a representative TEM micrograph.

The limited control over bidirectional ATRP of styrene to high molecular weights hampered reliable syntheses of microphase separated triblock copolymer samples with f_B < 0.40, thus limiting our ability to characterize samples with low f_B values. One such sample, SBS-28.6-27, displays a microphase separated morphology with a characteristic domain spacing d > 90 nm. This large domain spacing hampered SAXS analysis of this sample, thus precluding a definitive bulk morphological assignment. TEM analysis of polymer samples solvent cast from toluene and annealed for 24 h at 150 °C demonstrates the formation of a poorly ordered structure that could not be definitively assigned (Figure 6). Based on our morphological analyses and the sample composition, we tentatively assign the morphology as disordered spheres.

Disordered Cylinders Phase: f_B = 0.82. In contrast to the ordered phases observed at low values of f_B with high T_{ODT}s, SBS-25.4-82 exhibits poor long-range order and $T_{ODT} \sim 120$ °C as determined by temperature-dependent synchrotron SAXS (Figure 7). The azimuthally integrated SAXS intensity profile may be indexed to a cylindrical morphology, yet the broad

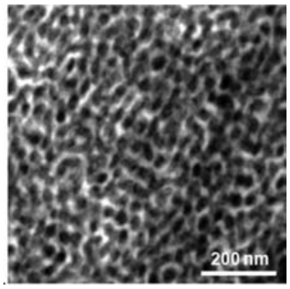

Figure 6. TEM micrograph of a sample of SBS-28.6-27 that was annealed for 24 h at 150 °C, showing a poorly ordered morphology tentatively assigned as disordered spheres based on polymer composition.

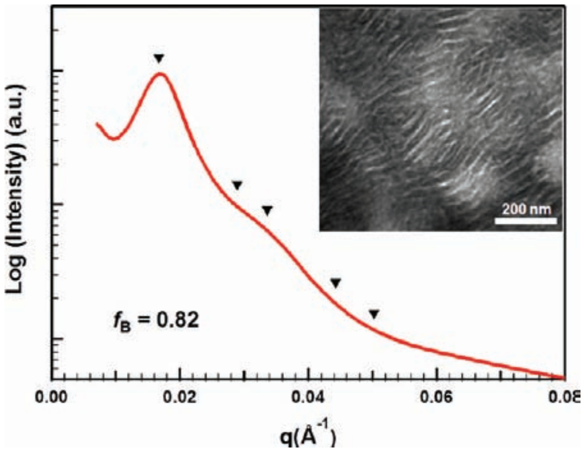

Figure 7. Azimuthally integrated synchrotron SAXS pattern for SBS-25.4-82 at 90 °C indexed to a morphology of hexagonally packed cylinders, with an inset showing a representative TEM micrograph of the rheometer-sheared sample cryo-sectioned normal to the shear-gradient ($\nabla \mathbf{v}$) direction (see text for details).

scattering maxima are symptomatic of a weakly segregated sample close to the order–disorder transition. A sample of this polymer was sheared in a parallel-plate rheometer at 115 °C at ω = 1.0 Hz for 10 min to orient the microdomains, followed by cryo-sectioning at −170 °C for TEM imaging along two axes: (1) normal to the shear direction (**v**), and (2) normal to the shear-gradient ($\nabla \mathbf{v}$) direction. TEM images of samples sectioned normal to the **v**-direction show only a random dispersion lacking any obvious order, while long thread-like structures are clearly seen in the samples sectioned normal to $\nabla \mathbf{v}$ (Figure 7 inset). These images suggest a morphology in which cylindrical polystyrene micelles lie in a matrix of poly(1,4-butadiene) with no long-range lattice order. The low degree of order at high f_B concurs with previous observations of weak lattice order, when the polydisperse block is the majority component in the melt.[48] We rationalize our result in terms of the inability of the wide range of molecular weights in the B block matrix of the cylindrical morphology to pack tightly enough to form a coherent, ordered morphology.

Polydisperse SBS Morphology Diagram. We summarize the results of our studies of polydisperse SBS triblock copolymers in Figure 8 as a $\chi_{SB}N$ versus f_B morphology diagram. In order to construct this phase portrait, we have assumed that the composition-independent $\chi_{SB}(T)$ takes the form

$$\chi_{SB}(T) = 30.137/T - 0.03813 \tag{1}$$

with respect to the 118 Å^3 monomer reference volume.[50] In contrast to the polydisperse SBS triblocks reported here that are comprised of perfectly regioregular 1,4-butadiene units arising from cyclic diolefin ROMP, this $\chi_{SB}(T)$ was determined using monodisperse SBS triblock copolymers containing ~7 mol % 1,2-butadiene units in the B block. We estimate that $\chi_{SB}(T)$ for the polydisperse SBS is ~12% higher than that calculated from eq 1 due to this difference in chain microstructure.[63] Consequently, the reported values of $\chi_{SB}N$ in Figure 8 underestimate the true segregation strengths. The location of the microphase separation transition (MST) above which ordered morphologies spontaneously form is estimated based on the location of T_{ODT} when accessible. The boundary depicted in Figure 8 otherwise represents an upper bound on the actual position of the MST, since $\chi_{SB}(T)$ α $(1/T)$. While this morphology diagram is constructed based on complete molecular and supramolecular characterization of seventeen samples, we cannot rule out the possibility that intermediate[42] and coexisting phases[64,65] may be observed at compositions not directly investigated in our studies.

In many cases, the order–disorder phase transition temperature T_{ODT} is higher than the polymer decomposition temperature (~ 220 °C). This precludes our ability to thermally disorder these copolymer samples by heating and to cool them into ordered equilibrium phases. Consequently, we have studied the morphologies of our copolymer samples after processing them by casting from a good solvent and thermal annealing, channel die alignment, and shearing in a parallel plate rheometer to induce the development of equilibrium morphologies.[42,66] The invariance of the observed morphologies under these various processing conditions suggests the equilibrium nature of these supramolecular structures. For a few samples, T_{ODT} was accessible and SAXS analyses were used to interrogate the disordered polymer melts. Above the accessible ODTs for SBS-19.2-61, SBS-29.1-65, and SBS-25.4-82, we observe only a single, broad SAXS peak that we assign to the correlation-hole scattering of a disordered copolymer melt[54] (see Supporting Information Figure S1). Note that this disordered melt scattering signature is distinctly different from the observed scattering from the disordered bicontinuous morphology. In general, temperature-dependent SAXS studies of polydisperse SBS copolymers did not reveal any order-to-order phase transitions between different supramolecular morphologies. Therefore, important qualitative trends in both the thermodynamic stabilities of the various microphase separated morphologies and the progression of observed phases are summarized in the morphology diagram presented in Figure 8.

Comparison of the locations of the phase windows for monodisperse SBS triblock copolymers with those of our polydisperse model system leads to the conclusion that the polydisperse B segment occupies a smaller volume than expected based on its number average molecular weight $M_{n,B}$ (*vide supra*). Upon careful consideration of the chain length and compositional polydispersities inherent in a continuously polydisperse SBS triblock copolymer, one finds that a substantial fraction of copolymer chains are comprised of very small B segments flanked on either side by monodisperse S blocks (Scheme 3). Below a critical B block molecular weight

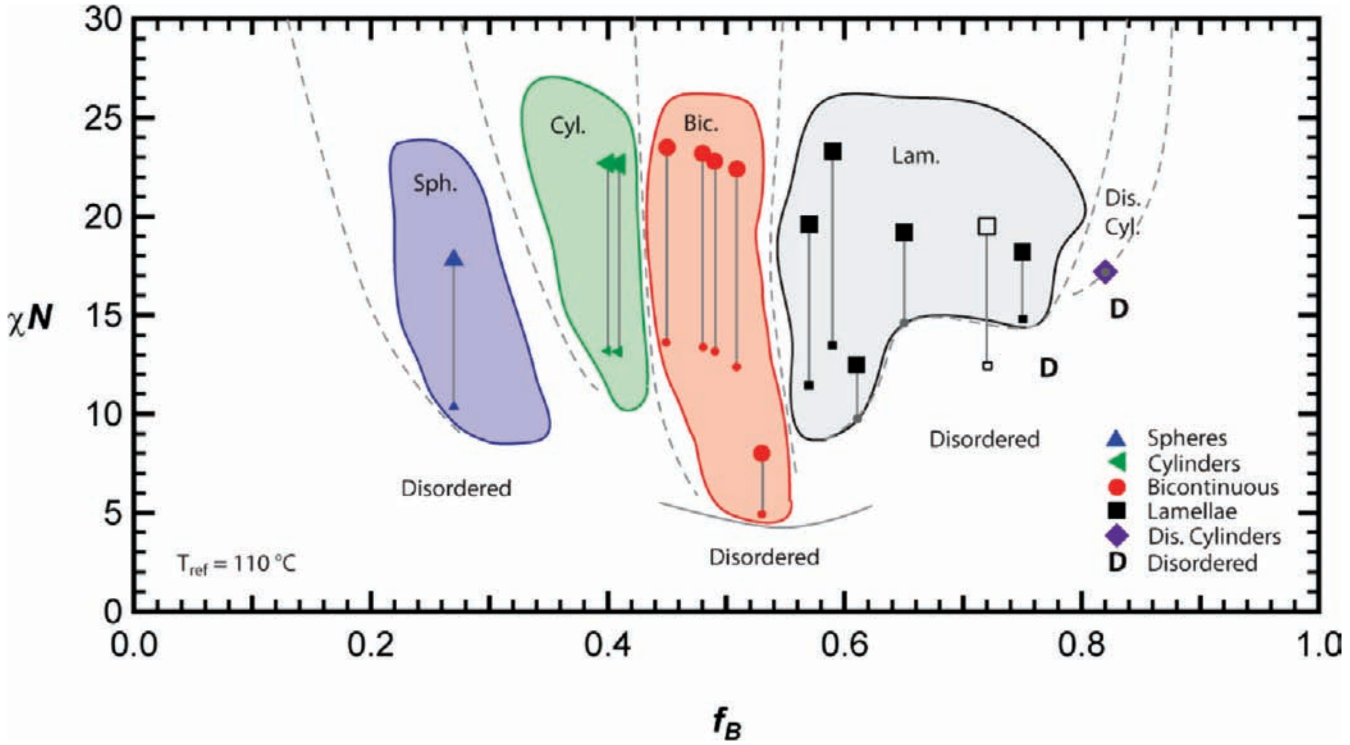

Figure 8. A χN versus f_B morphology diagram for SBS triblock copolymers with a polydisperse B block, showing a progression of phases with increasing f_B: spheres (blue, upward-pointing triangles), cylinders (green, left-pointed triangles), disordered bicontinuous (red circles), lamellae (black squares), and disordered cylinders (purple diamond). Points are plotted against χN at a reference temperature of 110 °C. Vertical lines (gray) mark the $\chi N(T)$ range over which a given morphology was observed up to T = 220 °C; gray circles indicate the location of an observed order−disorder transition. The unfilled marker denotes SBS-29.2-72, for which the S end blocks exhibit slightly broader polydispersities. Shaded areas and gray dotted lines outline the approximate locations of the morphology windows and their boundaries, respectively.

Scheme 3. Continuously Polydisperse Block Copolymers Exhibit Both Chain Length and Composition Polydispersities

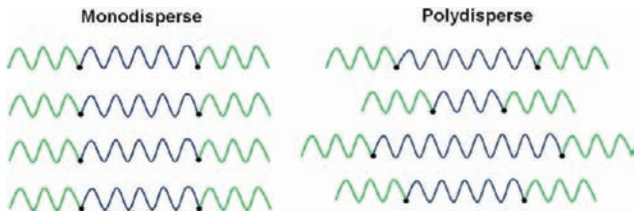

$M_{n,B}$ specified by the magnitude of χ_{SB}(T), these shorter chains desorb from the microphase separated interface and act as S−S homopolymer end block dimers that swell the S domains (Figure 9b).[45,67] This means that the physical volume filled by the polydisperse B block is smaller than one expects based on the chemical composition of the polymer quantified by f_B. The added presence of "S−S homopolymer" dimers increases the volume filled by the S domains, compounding the shifts in the phase windows toward high f_B. The desorption or release of "S−S homopolymers" from the domain interface increases the configurational entropy of the ensemble of chains, and thus the T_{ODT} for the polydisperse melt increases. By generalizing the calculation described by Lynd et al.[67] to determine the critical B block length below which a triblock copolymer may act like a homopolymer dimer, we find that disordered bicontinuous SBS-12.3-53 contains 26 wt % dimeric "S−S homopolymer" at 150 °C. Recalculation of the molecular weight distribution of the center poly(1,4-butadiene) block neglecting this "S−S

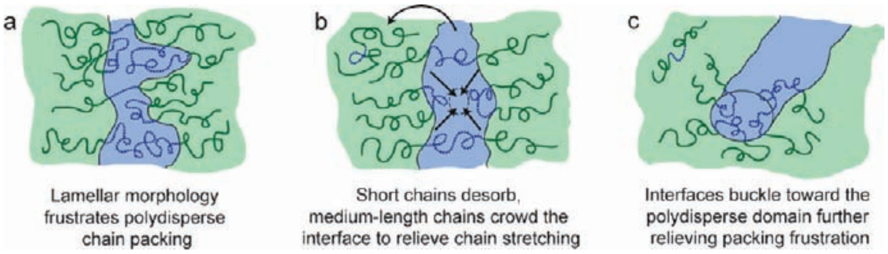

Figure 9. Schematic illustration of how chain length polydispersity in the center B blocks of ABA triblock copolymers results in (a) frustrated packing due to entropically unfavorable chain stretching resulting from incommensurate chain lengths. (b) In order to reduce this frustrated chain packing short B blocks desorb from the interface and S−S "homopolymer" dimers swell the S domains, while intermediate length chains crowd the domain interface and relieve chain stretching in the B block. (c) Consequently, the domain interfaces buckle toward the polydisperse domain, relieving chain stretching thereby entropically stabilizing the microphase separated state.

homopolymer" fraction shows that chain desorption reduces the B block polydispersity from M_w/M_n = 1.90 to 1.24, with a shift in the physical volume fraction from f_B = 0.53 to 0.39. Thus a polydisperse block copolymer behaves more like a binary blend of a relatively narrow dispersity ABA triblock swollen with a dimeric A–A homopolymer. Note that we never observed any signs of macrophase separation in the polydisperse triblock copolymer melts arising from the broad chain length distribution. This behavior differentiates the phase behavior of our continuously polydisperse materials from that of blends of monodisperse block copolymers having either variable compositions or molecular weights.[65,68,69]

The gain in configurational entropy of the microphase separated melt by release of "S–S homopolymer" from the interface is not the only factor contributing to the large T_{ODT} increases for polydisperse SBS copolymers. Among the chains that sit at the microphase separated domain interfaces, we speculate that copolymers with intermediate length B segments occupy interfacial area and shield copolymer chains with long B blocks from enthalpically unfavorable A monomer contacts (Figure 9b). Due to this "co-surfactant" effect of the intermediate length copolymers, chains with longer B blocks relax and this relief of B chain stretching increases the configurational entropy of the system.[15,45,70,71] This entropy gain further thermodynamically stabilizes the microphase separated melt, rendering T_{ODT} inaccessible at modest overall copolymer molecular weights. The relief of B chain stretching by interfacial crowding further reduces the volume filled by the polydisperse B block, causing even greater curvature of the microdomain interfaces toward the B domain (Figure 9c). Therefore, one observes a strong preference for the domain interfaces in polydisperse block copolymer melts to curve toward the polydisperse domain, attendant with shifts in the phase boundaries to higher polydisperse component volume fractions (f_B).[15,45]

The morphology diagram presented in Figure 8 for ABA triblock copolymers with a polydisperse interior B segment differs substantially from previous results on AB and BAB copolymers with polydisperse exterior B blocks. Studies of the latter copolymers reported the formation of only classical morphologies (Scheme 1) with modest thermodynamic stabilization of the microphase separated state.[14−16,48] Unlike the AB and BAB copolymers wherein the polydisperse B segment has one free end (Figure 1), the ABA chain topology constrains the polydisperse B segment at two domain interfaces with monodisperse A blocks (Figure 9). This chain connectivity constraint on the polydisperse B segments in ABA triblocks is absent in polydisperse AB and BAB copolymers with polydisperse B blocks. Therefore, the new, disordered bicontinuous morphology and the large thermodynamic stabilization of the microphase separated state must arise directly from embedding the polydisperse B segment in the interior of the ABA copolymer chain. The phase map presented here further suggests that the disordered bicontinuous morphology persists at lower molecular weights and higher temperatures than the lamellar samples with f_B = 0.61–0.65, which exhibit accessible order–disorder transition temperatures. More explicitly, the critical $\chi_{SB}N$ for microphase separation into lamellae (~9.5 for SBS-19.2-61) is apparently higher than that for the bicontinuous morphology, which persists even at $\chi_{SB}N$ = 4.5 (SBS-12.3-53). Enforcing a lamellar morphology for ABA triblock copolymers causes the chains to adopt conformations that either bridge three microphase separated domains or loop between two domains (Figure 9a).[72] The broad chain length distribution in the polydisperse center B segment likely frustrates chain packing in this layered structure. We suspect that low degrees of packing frustration cause subtle variations in the lamellar domain spacing, leading to the low degrees of translational order observed in the lamellar SBS samples. However, higher degrees of packing frustration may completely destabilize the lamellar phase (Figure 9b). The disordered bicontinuous morphology (Figure 4) permits irregular variations in the B domain sizes and shapes, wherein B chains of highly variable lengths may be readily incorporated into this microphase separated structure with concomitant relief of polymer chain stretching and packing frustration (Figure 9c). This relief of chain stretching entropically stabilizes the supramolecular assembly and may account for the apparent stability of the disordered bicontinuous phase. Ongoing studies aim to address the unusual morphological features of the disordered bicontinuous phase.

■ CONCLUSION

Investigations of the self-assembly behavior of poly(styrene-*block*-1,4-butadiene-*block*-styrene) (SBS) block copolymers comprised of a broad dispersity center poly(1,4-butadiene) block flanked by relatively narrow dispersity polystyrene end blocks revealed the unexpected ability of molecular heterogeneity to entropically stabilize these supramolecular assemblies. By studying the temperature-dependent phase behavior of a series of seventeen SBS triblock copolymer samples derived from tandem ROMP-ATRP syntheses, we demonstrated that center B block polydispersity causes very large shifts in the composition windows associated with the well-known morphologies as compared to the corresponding monodisperse triblock copolymers. The increased entropy associated with the incorporation of a broad distribution of molecular weights into the center block leads to entropic stabilization of the melt microphase separated structures through a conspiracy between short and long chains to fill space more efficiently and to relieve copolymer chain stretching in these self-assembled structures. These studies demonstrate the potential for tailoring block copolymer microphase separated morphologies and their thermodynamic stabilities, by tuning the polydispersities of the constituent homopolymer blocks. Additionally, relaxing the stringent constraint on copolymer dispersity opens opportunities to develop new nanostructured, functional block copolymers derived from monomers not amenable to controlled/living polymerizations.

■ ASSOCIATED CONTENT

Ⓢ Supporting Information

Detailed synthetic procedures and representative azimuthally integrated synchrotron X-ray diffraction patterns for SBS-29.1-65. This information is available free of charge via the Internet at http://pubs.acs.org.

■ AUTHOR INFORMATION

Corresponding Author

mahesh@chem.wisc.edu

Notes

The authors declare no competing financial interest.

ACKNOWLEDGMENTS

We gratefully acknowledge financial support from a National Science Foundation CAREER Award (DMR-0748503), the Donors of the American Chemical Society Petroleum Research Fund (ACS PRF 47143-G7), the UW-Madison NSF NSEC (DMR-0425880), and the University of Wisconsin−Madison. A.L.S. and K.I. acknowledge support from a NSF ACC-F postdoctoral fellowship (CHE-1041975) and a Korea Research Foundation postdoctoral fellowship (KRF-357-2008-C00097), respectively. This research relied upon NSF MRSEC and NSF NSEC core characterization facilities UW−Madison (DMR-0520527 and DMR-0425880). Portions of this work were also performed at the DuPont-Northwestern-Dow Collaborative Access Team (DND-CAT) located at Sector 5 of the Advanced Photon Source (APS), supported by E.I. DuPont de Nemours & Co., The Dow Chemical Company, and Northwestern University. Use of the APS, an Office of Science User Facility operated for the U.S. Department of Energy (DOE) Office of Science by Argonne National Laboratory, was supported by the U.S. DOE under Contract No. DE-AC02-06CH11357.

REFERENCES

(1) Whitesides, G. M.; Grzybowski, B. *Science* **2002**, *295*, 2418−2421.
(2) Redl, F. X.; Cho, K. S.; Murray, C. B.; O'Brien, S. *Nature* **2003**, *423*, 968−971.
(3) Li, Y.; Cai, W.; Duan, G. *Chem. Mater.* **2007**, *20*, 615−624.
(4) Miszta, K.; de Graaf, J.; Bertoni, G.; Dorfs, D.; Brescia, R.; Marras, S.; Ceseracciu, L.; Cingolani, R.; van Roij, R.; Dijkstra, M.; Manna, L. *Nat. Mater.* **2011**, *10*, 872−876.
(5) Bowden, N.; Terfort, A.; Carbeck, J.; Whitesides, G. M. *Science* **1997**, *276*, 233−235.
(6) Bowden, N. B.; Weck, M.; Choi, I. S.; Whitesides, G. M. *Acc. Chem. Res.* **2000**, *34*, 231−238.
(7) Antonietti, M.; Hartmann, J.; Neese, M.; Seifert, U. *Langmuir* **2000**, *16*, 7634−7639.
(8) Glotzer, S., C.; Solomon, M., J. *Nat. Mater.* **2007**, *6*, 557−562.
(9) Bates, F. S.; Fredrickson, G. H. *Phys. Today* **1999**, *52*, 32−38.
(10) Abetz, V.; Simon, P. F. W. *Adv. Polym. Sci.* **2005**, *190*, 125−212.
(11) Ruzette, A.-V.; Leibler, L. *Nat. Mater.* **2005**, *4*, 19−31.
(12) Bang, J.; Jeong, U.; Ryu, D. Y.; Russell, T. P.; Hawker, C. J. *Adv. Mater.* **2009**, *21*, 4769−4792.
(13) Bendejacq, D.; Ponsinet, V.; Joanicot, M.; Loo, Y. L.; Register, R. A. *Macromolecules* **2002**, *35*, 6645−6649.
(14) Ruzette, A.-V.; Tence-Girault, S.; Leibler, L.; Chauvin, F.; Bertin, D.; Guerret, O.; Gerard, P. *Macromolecules* **2006**, *39*, 5804−5814.
(15) Lynd, N. A.; Hillmyer, M. A. *Macromolecules* **2005**, *38*, 8803−8810.
(16) Lynd, N. A.; Meuler, A. J.; Hillmyer, M. A. *Prog. Polym. Sci.* **2008**, *33*, 875−893.
(17) Bates, F. S.; Fredrickson, G. H. *Annu. Rev. Phys. Chem.* **1990**, *41*, 525−57.
(18) Leibler, L. *Macromolecules* **1980**, *13*, 1602−17.
(19) Fredrickson, G. H.; Helfand, E. *J. Chem. Phys.* **1987**, *87*, 697−705.
(20) Cochran, E. W.; Garcia-Cervera, C. J.; Fredrickson, G. H. *Macromolecules* **2006**, *39*, 2449−2451.
(21) Tyler, C. A.; Morse, D. C. *Phys. Rev. Lett.* **2005**, *94*, 208302.
(22) Bates, F. S.; Schulz, M. F.; Khandpur, A. K.; Forster, S.; Rosedale, J. H.; Almdal, K.; Mortensen, K. *Faraday Discuss.* **1994**, *98*, 7−18.
(23) Davidock, D. A.; Hillmyer, M. A.; Lodge, T. P. *Macromolecules* **2003**, *36*, 4682−4685.
(24) Takenaka, M.; Wakada, T.; Akasaka, S.; Nishitsuji, S.; Saijo, K.; Shimizu, H.; Kim, M. I.; Hasegawa, H. *Macromolecules* **2007**, *40*, 4399−4402.
(25) Lee, S.; Bluemle, M. J.; Bates, F. S. *Science* **2010**, *330*, 349−353.
(26) Matsen, M. W.; Thompson, R. B. *J. Chem. Phys.* **1999**, *111*, 7139−7146.
(27) Mayes, A. M.; Olvera de la Cruz, M. *J. Chem. Phys.* **1989**, *91*, 7228−35.
(28) Hillmyer, M. A. *Curr. Opin. Solid State Mater. Sci.* **1999**, *4*, 559−564.
(29) Hawker, C. J.; Bosman, A. W.; Harth, E. *Chem. Rev.* **2001**, *101*, 3661−3688.
(30) Matyjaszewski, K.; Xia, J. *Chem. Rev.* **2001**, *101*, 2921−2990.
(31) Ouchi, M.; Terashima, T.; Sawamoto, M. *Chem. Rev.* **2009**, *109*, 4963−5050.
(32) Moad, G.; Rizzardo, E.; Thang, S. H. *Polymer* **2008**, *49*, 1079−1131.
(33) Bielawski, C. W.; Morita, T.; Grubbs, R. H. *Macromolecules* **2000**, *33*, 678−680.
(34) Pitet, L. M.; Amendt, M. A.; Hillmyer, M. A. *J. Am. Chem. Soc.* **2010**, *132*, 8230−8231.
(35) Pitet, L. M.; Hillmyer, M. A. *Macromolecules* **2009**, *42*, 3674−3680.
(36) Banik, S. M.; Monnot, B. L.; Weber, R. L.; Mahanthappa, M. K. *Macromolecules* **2011**, *44*, 7141−7148.
(37) Weber, R. L.; Ye, Y.; Schmitt, A. L.; Banik, S. M.; Elabd, Y. A.; Mahanthappa, M. K. *Macromolecules* **2011**, *44*, 5727−5735.
(38) Sriprom, W.; James, M.; Perrier, S.; Neto, C. *Macromolecules* **2009**, *42*, 3138−3146.
(39) Schmitt, A. L.; Mahanthappa, M. K. *Soft Matter* **2012**, *8*, 2294−2303.
(40) Matsushita, Y.; Noro, A.; Iinuma, M.; Suzuki, J.; Ohtani, H.; Takano, A. *Macromolecules* **2003**, *36*, 8074−8077.
(41) Hillmyer, M. A. *J. Polym. Sci., Part B: Polym. Phys.* **2007**, *45*, 3249−3251.
(42) Listak, J.; Jakubowski, W.; Mueller, L.; Plichta, A.; Matyjaszewski, K.; Bockstaller, M. R. *Macromolecules* **2008**, *41*, 5919−5927.
(43) Hustad, P. D.; Marchand, G. R.; Garcia-Meitin, E. I.; Roberts, P. L.; Weinhold, J. D. *Macromolecules* **2009**, *42*, 3788−3794.
(44) Meuler, A. J.; Ellison, C. J.; Qin, J.; Evans, C. M.; Hillmyer, M. A.; Bates, F. S. *J. Chem. Phys.* **2009**, *130*, 234903−234919.
(45) Beardsley, T. M.; Matsen, M. W. *Macromolecules* **2011**, *44*, 6209−6219.
(46) Li, S.; Register, R. A.; Landes, B. G.; Hustad, P. D.; Weinhold, J. D. *Macromolecules* **2010**, *43*, 4761−4770.
(47) Meuler, A. J.; Ellison, C. J.; Hillmyer, M. A.; Bates, F. S. *Macromolecules* **2008**, *41*, 6272−6275.
(48) Lynd, N. A.; Hillmyer, M. A. *Macromolecules* **2007**, *40*, 8050−8055.
(49) Mahanthappa, M. K.; Bates, F. S.; Hillmyer, M. A. *Macromolecules* **2005**, *38*, 7890−7894.
(50) Widin, J. M.; Schmitt, A. K.; Im, K.; Schmitt, A. L.; Mahanthappa, M. K. *Macromolecules* **2010**, *43*, 7913−7915.
(51) Fetters, L. J.; Lohse, D. J.; Richter, D.; Witten, T. A.; Zirkel, A. *Macromolecules* **1994**, *27*, 4639−4647.
(52) Bielawski, C. W.; Hillmyer, M. A. In *Handbook of Metathesis*; Grubbs, R. H., Ed.; Wiley-VCH: Weinheim, Germany, 2003; Vol. 3, pp 255−281.
(53) Ji, S.; Hoye, T. R.; Macosko, C. W. *Macromolecules* **2004**, *37*, 5485−5489.
(54) Bates, F. S. *Macromolecules* **1985**, *18*, 525−528.
(55) Roe, R.-J. *Methods of X-Ray and Neutron Scattering in Polymer Science*; Oxford University Press: New York, 2000.
(56) Mai, S.-M.; Mingvanish, W.; Turner, S. C.; Chaibundit, C.; Fairclough, J. P. A; Heatley, F.; Matsen, M. W.; Ryan, A. J.; Booth, C. *Macromolecules* **2000**, *33*, 5124−5130.
(57) Lynd, N. A.; Hamilton, B. D.; Hillmyer, M. A. *J. Polym. Sci., Part B: Polym. Phys.* **2007**, *45*, 3386−3393.
(58) Arriola, D. J.; Carnahan, E. M.; Hustad, P. D.; Kuhlman, R. L.; Wenzel, T. T. *Science* **2006**, *312*, 714−719.

(59) Bates, F. S.; Maurer, W. W.; Lipic, P. M.; Hillmyer, M. A.; Almdal, K.; Mortensen, K.; Fredrickson, G. H.; Lodge, T. P. *Phys. Rev. Lett.* **1997**, *79*, 849−852.

(60) Ellison, C. J.; Meuler, A. J.; Qin, J.; Evans, C. M.; Wolf, L. M.; Bates, F. S. *J. Phys. Chem. B* **2009**, *113*, 3726−3737.

(61) Thompson, R. B.; Matsen, M. W. *Phys. Rev. Lett.* **2000**, *85*, 670−673.

(62) Wagner, N. L.; Timmers, F. J.; Arriola, D. J.; Jueptner, G.; Landes, B. G. *Macrmol. Rapid. Commun.* **2008**, *29*, 1438−1443.

(63) Frielinghaus, H.; Schwahn, D.; Willner, L. *Macromolecules* **2001**, *34*, 1751−1763.

(64) Listak, J.; Jia, X.; Plichta, A.; Zhong, M.; Matyjaszewski, K.; Bockstaller, M. R. *J. Polym. Sci., Part B: Polym. Phys.* **2012**, *50*, 106−116.

(65) Matsen, M. W. *Phys. Rev. Lett.* **2007**, *99*, 148304−148307.

(66) Zalusky, A. S.; Olayo-Valles, R.; Wolf, J. H.; Hillmyer, M. A. *J. Am. Chem. Soc.* **2002**, *124*, 12761−12773.

(67) Lynd, N. A.; Hillmyer, M. A.; Matsen, M. W. *Macromolecules* **2008**, *41*, 4531−4533.

(68) Noro, A.; Iinuma, M.; Suzuki, J.; Takano, A.; Matsushita, Y. *Macromolecules* **2004**, *37*, 3804−3808.

(69) Noro, A.; Cho, D.; Takano, A.; Matsushita, Y. *Macromolecules* **2005**, *38*, 4371−4376.

(70) Court, F.; Hashimoto, T. *Macromolecules* **2002**, *35*, 2566−2575.

(71) Court, F.; Yamaguchi, D.; Hashimoto, T. *Macromolecules* **2006**, *39*, 2596−2605.

(72) Drolet, F.; Fredrickson, G. H. *Macromolecules* **2001**, *34*, 5317−5324.